Phytochemical Insights and Antimicrobial Efficacy of *Cocculus hirsutus* Against Diabetic Wound Infections

Calista Stephanie A[1], Nandhini R[1], Anugraha J[2], Vyshali S[2] & Dr. T. Sharmila Raj[1*]

[1,2,1*] *Department of Biotechnology, Sri Shakthi Institute of Engineering and Technology, Coimbatore, TN*

Corresponding Author

Dr. T. Sharmila Raj

Assistant Professor, Department of Biotechnology, Sri Shakthi Institute of Engineering and Technology, Email: sharmilapsg20@gmail.com

Abstract

This study investigates the phytochemical composition and pharmacological potential of Cocculus hirsutus, a medicinal plant traditionally utilised for its diverse therapeutic properties. Qualitative phytochemical screening revealed the presence of phenols, saponins, tannins, quinones, proteins, glycosides, and terpenoids, while flavonoids, alkaloids, and steroids were notably absent. To analyse the anti-microbial like MIC, MBC, and Biofilm, mode of action like hydrophobicity, membrane stability, toxin neutralisation for the diabetic wound infection. To evaluate the bioactive potential of these bioactive compounds, molecular docking studies were performed against six receptors to understand the mechanism of antibacterial and antidiabetic activity. The study found that the ligands, such as Phenytoin, Lupeol, and Butorphanol, showed strong binding affinities with the bioactive compounds. Moreover, ADMET and ProTox studies were also performed to understand the pharmacokinetic properties and toxicity of these bioactive compounds, indicating that they have good potential to act as an effective drug for diabetic wound infection. C. hirsutus is found to be rich in bioactive secondary metabolites with good potential to be used as an effective drug for wound infection.

KEY WORDS: *Cocculus hirsutus, Anti-microbial, Mode of action, Phenytoin, ADMET and ProTox*

1. Introduction

Diabetic wound infections are one of the fastest-spreading problems among the diabetic people. Each year, about 26 million new diabetic foot ulcers and wound infections pop up globally, and the chance of getting one in your lifetime sits somewhere between 15% and 25% (Mottola et al., 2020; Darvishi et al., 2022). These infections can turn wounds chronic, lead to non-curable, and even threaten lives. All that adds up to a big burden for healthcare and pushes mortality rates up. Diabetes makes people more vulnerable for a few reasons: their immune response drops, blood vessels get damaged, and blood sugar stays high. This creates the perfect storm for all kinds of microbes to settle in and take over. The microorganisms behind infections *Staphylococcus aureus, Pseudomonas aeruginosa, Klebsiella pneumoniae, Acinetobacter baumannii, Enterococcus faecalis*, and *Streptococcus pneumoniae* will form stubborn biofilms for their protection. That makes them tough to fight, as these biofilms boost their resistance to antibiotics (Anita et al., 2023; Mottola et al., 2020). The rise of multidrug-resistant

strains really limits treatment options, so finding new, effective antimicrobial agents especially from plants—just feels urgent right now. Medicinal plants have played a huge role in traditional healing and infection systems with their phytochemicals things like phenolic acids, tannins, saponins, terpenoids, and glycosides have shown broad antimicrobial, anti-inflammatory, antioxidant, and antidiabetic powers (Yunitasari et al., 2022; Ramya et al., 2019). Among all the traditional remedies out there, *Cocculus hirsutus*, climbing plant grows fast and shows up in India, Pakistan, Sri Lanka, Bangladesh, Myanmar, and parts of Africa. It's a staple in Ayurvedic and folk medicine, used for fevers, skin and urinary infections, diabetes, jaundice, rheumatism, and as a general tonic (Logesh et al., 2020; Nayak and Singhai, 2003). *Cocculus hirsutus* packs a punch with bioactive alkaloids, flavonoids, triterpenoids, and phenolic acids (Logesh et al., 2020; Abbagoni et al., 2021). Earlier studies on *C. hirsutus* have shown it fights both Gram-positive and Gram-negative bacteria *Staphylococcus aureus, Pseudomonas aeruginosa, Escherichia coli* and even has antidiabetic, antioxidant, and wound-healing abilities (Nayak and Singhai, 2003; Kalirajan et al., 2011; Badole et al., 2006). But no one really digs into how its compounds block biofilm formation, how they work against infectious agents, or their potential using in silico (computer-based) methods for diabetic wound pathogens. That gap matters, especially since biofilms from MDR bugs are now known to be the biggest obstacle sticking around in chronic diabetic ulcers. These biofilms make bacteria up to 1000 times more tolerant to antibiotics than in their free-floating form (Mottola et al., 2020; Darvishi et al., 2022). Molecular docking is a gamechanger in today's drug discovery. It lets researchers quickly and cheaply screens plant-based compounds against target proteins, giving insight into how those compounds interact (Meng et al., 2011; Thamaraiselvi et al., 2021). Paired with ADMET prediction tools like pkCSM and ProTox-II, in silico approaches can map out a drug's profile early on—saving time and money (Nasr et al., 2022; Marta et al., 2019). Blocking α-amylase, which helps break down carbs and absorbs glucose after meals, is a well-known way to treat type 2 diabetes. In fact, many plant extracts that block this enzyme show promising antidiabetic activity (Yunitasari et al., 2022; Suaeda maritima study, 2023). So, this study set out to scientifically check the phytochemical content and pharmacological potential of Cocculus hirsutus leaf ethanol extract for tackling diabetic wound infections. The researchers ran qualitative phytochemical screening, GC-MS analysis, tested antidiabetic power via alpha-amylase inhibition, checked antimicrobial activity by MIC and MBC against human pathogens, measured biofilm inhibition, and looked at how it works testing cell hydrophobicity, membrane stability, and toxin neutralization. They also did molecular docking with the bioactive compounds against pathogen receptors, then followed up with ADMET and ProTox-II studies. Basically, this work backs up folk wisdom with actual science and could lead to new therapies for diabetic wound infections (Logesh et al., 2020; Elshikh et al., 2016).

2. Materials and method

2.1 Materials

The *Cocculus hirsutus* leaves were collected from local area in Coimbatore, India. Chemicals used were nutrient broth, nutrient agar, ethanol, Resazurin dye, NaCl, KCl, KH_2PO_4, Na_2HPO_4, amylase, starch, crystalline violet, PBS, SDS, Triton, Toluene, Biuret reagent, etc., which were procured from Synthesis Chemical.

2.2 *Cocculus hirsutus*

The *Cocculus hirsutus* powder was mixed with ethanol and heated on a heating mantle until the volume reduced. The extract was filtered through Whatman No. 1 filter paper and stored at 4°C until further use.

Figure 1: Extraction of sample

2.3 Phytochemical analysis

Qualitative tests for phytochemicals in the plant extract were carried out to analyze for the presence of various phytochemicals in the plant extract. The presence of phenolic compounds was checked by mixing 1 ml of the extract with 1% ferric chloride ($FeCl_3$) solution. The presence of phenolic compounds was indicated by the formation of a green or black color (Yunitasari N et al., 2022) (Lourence et al., 2024). The presence of flavonoids was checked by adding 1 ml of 1% sodium hydroxide (NaOH) solution to 1 ml of the extract. The presence of flavonoids was indicated by the formation of a green or yellow color (Ramya et al., 2019). The presence of saponins was checked by mixing 1 ml of the extract with 3 ml of distilled water and then shaking it vigorously. The presence of saponins was indicated by persistent foam formation (Ramya et al., 2019) (Lourence et al., 2024). The presence of tannins was checked by mixing 1 ml of the extract with 1 ml of bromine water. The presence of tannins was indicated by the formation of a green or brown colour (Wiraswati et al., 2024). Qualitative phytochemical analysis of the plant extract was performed to identify the presence of various secondary metabolites using standard colorimetric methods. For phenolic compounds, mixing 1 ml of the extract with 1% ferric chloride, where the solution turned off a green or black coloration was taken as a positive result (Yunitasari N et al., 2022) (Lourence et al., 2024). Flavonoids were identified by the addition of 1 ml of 1% sodium hydroxide (NaOH) to 1 ml of the extract, with the appearance of a green or yellow coloration indicating a positive result (Ramya et al., 2019). Saponins were detected by mixing 1 ml of the extract with 3 ml of distilled water followed by vigorous shaking, where persistent foam formation was considered indicative of their presence (Ramya et al., 2019) (Lourence et al., 2024). The presence of tannins was assessed by mixing 1 ml of the extract with 1 ml of bromine water, with a color change to green or brown indicating a positive result (Wiraswati et al., 2024). Alkaloids were detected by treating 1 ml of the extract with 1 ml of iodine solution, where the development of a brown coloration was taken as a positive indication (Lourence et al., 2024). Quinones were identified by the addition of 1 ml of hydrochloric acid (HCl) to 1 ml of the extract, with a green coloration indicating their presence (Yunitasari N et al., 2022). Proteins were detected using the xanthoproteic test, wherein 1 ml of the extract was treated with 1 ml of concentrated nitric acid, and the appearance of a golden yellow color was recorded as a positive result (Godlewska et a.,2023). Glycosides were identified by sequentially mixing 1 ml of the extract with 1 ml each of chloroform, glacial acetic acid, 1% $FeCl_3$, and concentrated sulfuric acid (H_2SO_4), where the formation of a green and black layered coloration indicated their presence (Ramya et al., 2019). Steroids and terpenoids were both detected using a similar Liebermann–Burchard and Salkowski test approach, respectively, wherein 1 ml of the extract was mixed with 1 ml each of chloroform, glacial acetic acid, and concentrated H_2SO_4; the development of a brown to yellow coloration indicated the presence of steroids, while a violet or pink coloration was taken as indicative of terpenoids (S. Sazada et al., 2009) (Samar et al., 2022).

2.4 Anti-diabetic test

2.4.1 Preparation of reagents

Phosphate-Buffered Saline (PBS): Phosphate-buffered saline (PBS) was used as the reaction medium throughout the assay. PBS (100 ml) was prepared by dissolving sodium chloride (NaCl, 0.8 g), potassium chloride (KCl, 0.3 g), potassium dihydrogen phosphate (KH_2PO_4, 0.02 g), and disodium hydrogen phosphate (Na_2HPO_4, 0.2 g) in an appropriate volume of distilled water. The solution was mixed thoroughly, and the final volume was adjusted to 100 ml using distilled water.

Enzyme Solution: The α-amylase enzyme solution was prepared by dissolving 0.2 g of α-amylase in 25 ml of PBS. The solution was gently mixed until complete dissolution was achieved and stored appropriately until required for the assay.

Starch Substrate Solution: The substrate solution was prepared by dissolving 0.1 g of soluble starch in 25 ml of distilled water. The mixture was subjected to gentle heating with continuous stirring to ensure complete and uniform dissolution of the starch prior to use.

3,5-Dinitrosalicylic Acid (DNS) Reagent: The DNS color-developing reagent was prepared by combining two separately prepared solutions. Solution A was prepared by dissolving an appropriate quantity of sodium hydroxide (NaOH) in 20 ml of distilled water to obtain a 2 M concentration. Solution B was prepared by dissolving DNS (0.5 g) and sodium potassium tartrate tetrahydrate ($C_4H_4KNaO_6 \cdot 4H_2O$, 30 g) in distilled water. Solutions A and B were subsequently combined and mixed thoroughly to obtain the working DNS reagent.

2.4.2 α-Amylase inhibition assay procedure

The α-amylase inhibition assay of the prickly pear samples was conducted using the DNS colorimetric method. The test sample of the desired concentration was placed in a test tube, followed by the addition of 200 µl of α-amylase enzyme solution and 200 µl of PBS solution. The mixture was then incubated at 37°C for 20 minutes to allow sufficient interaction between the enzyme and the inhibitor in the test sample. After the completion of the incubation period, 200 µl of starch substrate solution was added to the mixture to initiate the enzymatic reaction, which was then incubated at 37°C for a specific period. The reaction was terminated by adding 2 ml of DNS solution to the mixture. The α-amylase inhibitory activity of the test samples was conducted using the DNS colorimetric method. For this purpose, the test sample of the desired concentration was placed in a reaction tube, followed by the addition of 200 µl of the prepared α-amylase enzyme solution and 200 µl of PBS solution. The mixture was then incubated at 37°C for 20 minutes to allow sufficient interaction between the enzyme and the inhibitor in the sample. After the completion of the incubation period, 200 µl of starch substrate solution was added to the mixture to initiate the enzymatic reaction, which was then incubated at 37°C for a specific period. The reaction was terminated by adding 2 ml of DNS solution to the mixture. The mixture was then heated in a boiling water bath at 100°C for 15 minutes to help the color develop, which corresponds to the amount of maltose released when starch is broken down by enzymatic hydrolysis. After that, we measured the absorbance of each reaction mixture at 540 nm with a UV-Vis spectrophotometer at room temperature. For the control reaction, we swapped out the test sample and used the same volume of the matching solvent instead. Acarbose, an α-amylase inhibitor, was used as the positive control. All experiments were run three times, and the results are reported as the mean plus or minus the standard deviation (SD). (Yunitasari N et al., 2022)

$$\text{Inhibition (\%)} = \frac{\text{Blank OD Value} - \text{Sample OD Value}}{\text{Blank OD Value}} * 100$$

2.5 Anti-microbial activity

2.5.1 MIC (Minimal Inhibitory Concentration)

Sterile nutrient broth was prepared and 100 µl of it was added to each well of a sterile 96 wells microlitre plate. 100 µl of the sample was placed into the first well, then it was diluted step by step across the wells in the same row. This process was done for each test organism. Next, 10 µl of the microorganism inoculum was pipetted into each well, and then the resazurin indicator was added. The plates were incubated at 37°C for 24 hours. The change from blue violet to pink indicated microorganism growth, whereas no colour change indicated inhibition of growth. (Elshikh et al., 2016).

2.5.2 MBC (Minimum Bactericidal Concentration)

Nutrient agar was made and sterilized using aseptic technique, then poured into sterile petri dishes and left to solidify. The plates were then treated with the sample at concentrations that matched the MIC values determined. At the concentrations the MBC were tested. The result shows no obvious microbial growth or any inhibition zones, which suggests the sample didn't show antimicrobial activity under those test conditions. (Elshikh et al., 2016)

2.5.3 Biofilm formation analysis

The nutrient broth (3 ml) was prepared in each test tube, which was sterilized. After the test tubes had cooled to room temperature, 100 µl of microbial culture was added to each test tube, followed by the addition of the sample in concentrations equivalent to the previously determined MIC. The test tubes were then incubated at 37°C for 24 hours to obtain biofilm formation. The culture was discarded, and 1 ml of crystal violet solution was added to each test tube for staining. After 10 min of incubation at room temperature, the test tubes were rinsed three times with 3 ml of distilled water to remove excess stain, followed by air-drying. Biofilm formation was determined by measuring the absorbance at 540 nm using a digital colorimeter. (Suganya et al., 2021)

$$\text{Biofilm test (\%)} = \frac{(\text{Untreated} - \text{Treated})}{\text{Untraeted}} * 100$$

$$\text{Biofilm test (\%)} = \frac{(X\% + Y\% + Z\%)}{3}$$

2.6 Mode of action

2.6.1 Surface hydrophobicity assay

Nutrient broth (5ml) was prepared and then sterilized in each test tube. Once cooled to room temperature, 100µl of the microbial culture was added to each test tube. Then the sample was added at each concentration to the tubes in accordance with the result from MIC test. All test tubes were left in incubation at 37°C for 24 hours. After 24 hours incubation, centrifuged the broth culture at 10000rpm for 2min. Remove the supernatant and the pellet re-suspended in 1ml of PBS to obtain optical density (620nm). Add 1ml of toluene and invert gently 2-3 times, then keep it aside without disturbing the contents for 5-10 min for phase separation. When 2 layers were well defined, top layer was discarded and optical density (620nm) of bottom layer was determined using digital colorimeter (Selvaraj et al., 2020) (Rosenberg., 2006).

$$\text{Hydrophobicity (\%)} = \frac{0.3 - sample\ OD}{0.3} * 100$$

2.6.2 Membrane stability

5mL of nutrient broth was pipetted into test tubes and sterilised. Once cooled to room temperature, tubes were inoculated with 100ml of the cultured bacteria and incubated at 37°C for 24 hours. The cultures were then transferred in to centrifuge tubes and centrifuged at 10,000rpm for 2min, and the supernatants discarded for the pellet. the pellet was re suspended in 1ml of phosphate buffered saline (PBS) and mixed well. The test sample was added to the suspension for the treated group while the untreated group was used as a control, and the tubes incubated at 37°C for 30min. The suspension was then centrifuged at 10,000rpm for 2min and the supernatant discarded before resuspending the pellet in 1ml PBS, then 1ml of 0.15% sodium dodecyl sulfate (SDS) was added and mixed, and the optical density OD was recorded at 565nm at 0,2,4,6,8 and 10min. A blank of 1ml PBS with 1ml of 0.15% SDS was used for baseline correction (Reddy et al, 2014).

2.6.3 Toxin neutralization

Test tubes were then filled with 5ml of sterile nutrient broth and sterilized. The test tubes were then cooled to room temperature and in each tube 100ml of culture was introduced. The test sample was introduced at levels consistent with the MIC values. The test tubes were then incubated at 37°C for 24 hours. Following incubation, the test tubes were then spin in a centrifuge set at 10000 rpm for 2 min while supernatant was collected and the rest discarded. For the haemolytic assay, positive and negative controls were prepared. Positive control- 1.5 ml of phosphate buffered saline (PBS) + 1.5 ml of blood suspension. Negative control- 1.5 ml of Triton X-100 + 1.5 ml of blood suspension. 1.5 ml of the collected supernatant (treated and untreated) was added to 1.5 ml blood suspension in a separate test tube. Both test tubes were incubated at 37°C for 24 hours and centrifuged at 10,000 rpm for 2 min. The supernatant was collected and absorbance was determined against 541 nm. The zero of the spectrophotometers was adjusted with PBS. (Esnaashari et al., 2023)

$$\text{Hemolysis inhibition (\%)} = \frac{\text{Untreated OD Value} - \text{Treated OD Value}}{\text{Untreated OD Value}} * 100$$

2.7 Docking

The molecular docking was performed using PyRx and Discovery Studio. The receptors of the microorganisms were retrieved from the Protein Data Bank (PDB) database. The receptors were downloaded in Legacy PDB format. The receptor structure was organized by removing the water, hetatm and ligand groups. Under chemistry section, hydrogen and polar compounds are added to the receptor. In the CASTp, the chains and Seq ID of the receptors are noted. In the PyRx, the receptor is loaded and made it into a macromolecule. In the Open Babel, ligands were inserted which was downloaded from the PubChem. All ligands underwent energy minimization before docking to obtain stable conformations. After the grid formation, docking is run. The csv format result is downloaded and used for further process. (Marta et al.,2019)

2.8 Toxicity analysis

In the ProTox-II approach, their toxicology profiles, including acute toxicity, hepatotoxicity, cytotoxicity, carcinogenicity, mutagenicity, and immunotoxicity, among other toxicology endpoints. The molecular features for the chemicals were then obtained through a range of methods, including similarity analysis, pharmacophore modelling, and fragment propensity evaluation, among other approaches, to determine the structural characteristics that are responsible for the toxicity of the chemicals. The obtained features were then used to train machine learning models, primarily a random forest classifier, whose performance was validated and improved to ensure high prediction accuracy. The workflow for the web server is such that users can input a chemical structure, for example, through a SMILES string, and then the prediction for the toxicity is obtained, including the descriptors, simultaneously for multiple toxicology endpoints. The output is a comprehensive prediction that includes the toxicity class, LD50, and probability score, among other results. The performance of the model was validated internally and using an independent dataset, including the use of accuracy, sensitivity, specificity, and receiver operating characteristic curve analysis. The models are then integrated into a web server that is easy to use, such that researchers can use the tool to efficiently perform toxicity prediction, eliminating the need for animal testing and making the approach useful for early-stage drug discovery and development.

2.9 pkCSM

In the pkCSM study, the approach taken was the development of a predictive system of pharmacokinetics and toxicity based on the use of graph-based signatures of small molecules. This approach was taken by first developing large datasets of compounds with experimentally validated pharmacokinetic and toxicity properties, including absorption, distribution, metabolism, excretion, and toxicity (ADMET) endpoints. Each of these compounds was represented as a graph, with atoms represented as nodes and bonds represented as edges. Distance-based graph signatures were then calculated and used as input to machine learning algorithms, primarily random forest methods, which were then trained on the dataset to make predictions of quantitative and qualitative properties of the compounds. This approach was validated using cross-validation and test set methods and evaluated according to accuracy, sensitivity, specificity, and the use of the ROC curve. This approach can now be implemented as a tool in which the user can input the chemical structure of a molecule in a variety of formats, including the use of the SMILES string format, and the pkCSM tool can then generate predictions of multiple ADMET endpoints simultaneously. This tool has now been implemented as a webserver and can thus be used by researchers to determine the potential of a candidate molecule to be a viable drug candidate according to several criteria.

3. Result and discussion

3.1 Phytochemical analysis

From the qualitative phytochemical screening of *Cocculus hirsutus* whose results are shown in Table 1 and Figure 2, it was observed that Phenols, saponins, tannins, quinones, proteins, glycosides and terpenoids are

present. Flavonoids, alkaloids and steroids were not present in the extract. Presence of these compounds revealed that *C. hirsutus* could possibly be exploited as a potential source of bioactive secondary metabolites.

Table 1: Phytochemical analysis of *Cocculus hirsutus*

S.no	Phytochemical analysis	Result
1	Phenol	+
2	Flavonoids	-
3	Saponins	+
4	Tannins	+
5	Alkaloids	-
6	Quinones	+
7	Protein	+
8	Glycosides	+
9	Steroids	-
10	Terpenoids	+

Figure 2: Phytochemical analysis of *Cocculus hirsutus*

3.2 GC-MS

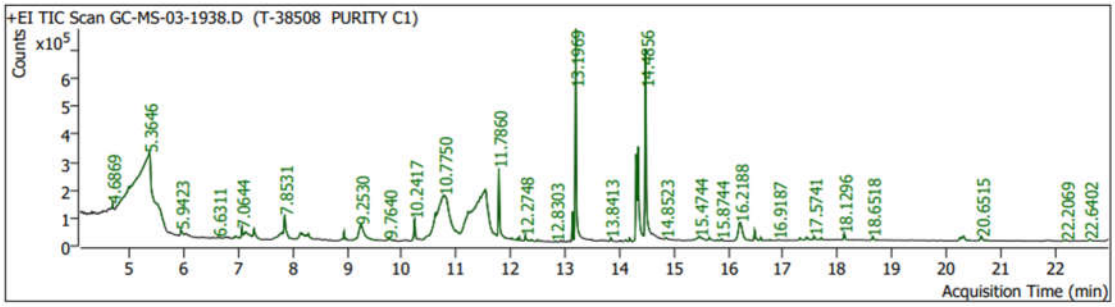

Figure 3: GC-MS for *Cocculus hirsutus*

Glycerine had the greatest area count of around 27.6%, as seen in the above Figure 3 and which will help in moisture retention and tissue regeneration. Inositol, 1-deoxy was identified at around 20.9% and Myo-inositol, 4-C-methyl at around 15.6%. Inositol in formula has cell growth and membrane repair

properties. For the FA studies, Octadecanoic acid was detected at around 6.8%, n-Hexadecenoic acid by 5.8% and cis-Vaccenic acid at around 5.8%. These have anti-inflammatory and anti-microbial activity that is present in wound infection control.

3.3 Anti-diabetic assay

The anti-diabetic activity (observed inhibition) of the aqueous extract of *Cocculus hirsutus* (Kattukodi) was determined at doses of 25, 50, 75, 100, 250, 500 and 1000 g/ml., illustrated in Table 2 and Figure 4. The aqueous extract showed a dose-dependent variation in inhibition over the test concentrations. The percentage inhibition was again highest at 75 g/ml (61.80%, indicating the best response at this level, followed by a moderate response at 100 g/ml (48.87%). Lower inhibition was observed at the concentrations 25, 50, 250, 500 and 100 g/ml (0.8833%, 3.2835%, 2.4651%, 2.72066%, 4.547%) respectively. The mean percentage inhibition across the concentrations was 36.66 ± 12.77%, suggesting that, relative to the other extracts tested, this aqueous extract shows a tendency towards moderate anti-diabetic activity in terms of its ability to which appears to act via the modulation of glucose metabolising activities.

Table 2: Anti-diabetic activity of *Cocculus hirsutus* extract at different concentrations

S.no	Concentration (µg/ml)	Inhibition (%) (Mean ± SD (0.1))
1	25	0.089
2	50	0.449
3	75	0.449
4	100	0.449
5	250	1.841
6	500	1.931
7	750	2.111
8	1000	2.201

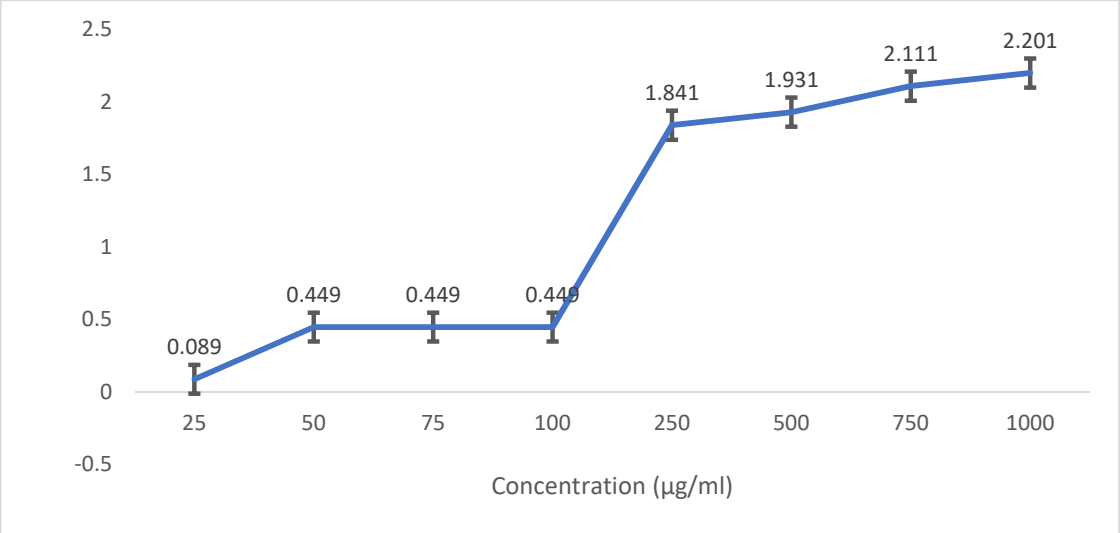

Figure 4: Inhibitory activity (%) of *Cocculus hirsutus* extract at different concentrations in α-amylase inhibition assay.

3.4 Anti-microbial activity

The antimicrobial activity of the *Cocculus hirsutus* extract as shown in Figures 5 and 6 was tested by Minimal Inhibitory Concentration (MIC) assay. The change from blue violet to pink indicated microorganism growth, whereas no colour change indicated inhibition of growth inhibition. According to the Table 3 it is showed that we got different MIC values.

It is proved that sample shows inhibition in 1st well for all the test organism which is 100 µg/ml. Followingly the MBC analysis was done to prove there is no growth of any microorganism which shows the sample kills the bacteria and doesn't allow it to grow.

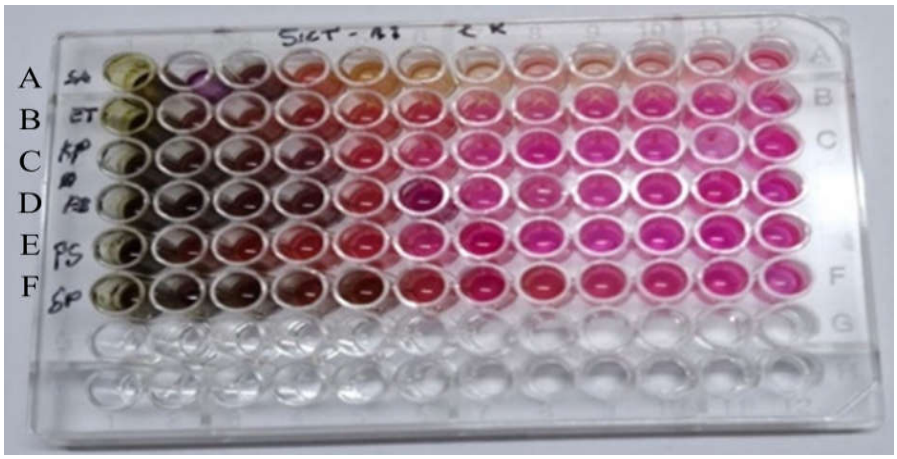

Figure 5: Determination of minimum inhibitory concentration (MIC) of *Cocculus hirsutus* extract using microdilution assay, showing visible color change indicative of microbial growth across tested concentrations.

Table 3: MIC and MBC of *Cocculus hirsutus* extract showing no antimicrobial activity at the tested concentration

S. no.	Microorganisms	Concentration (µg/ml)
1	A *Staphylococcus aureus*	100
2	B *Enterococcus faecalis*	100
3	C *Klebsiella pneumoniae*	100
4	D *Acinetobacter baumannii*	100
5	E *Pseudomonas areuginosa*	100
6	F *Streptococcus pneumoniae*	100

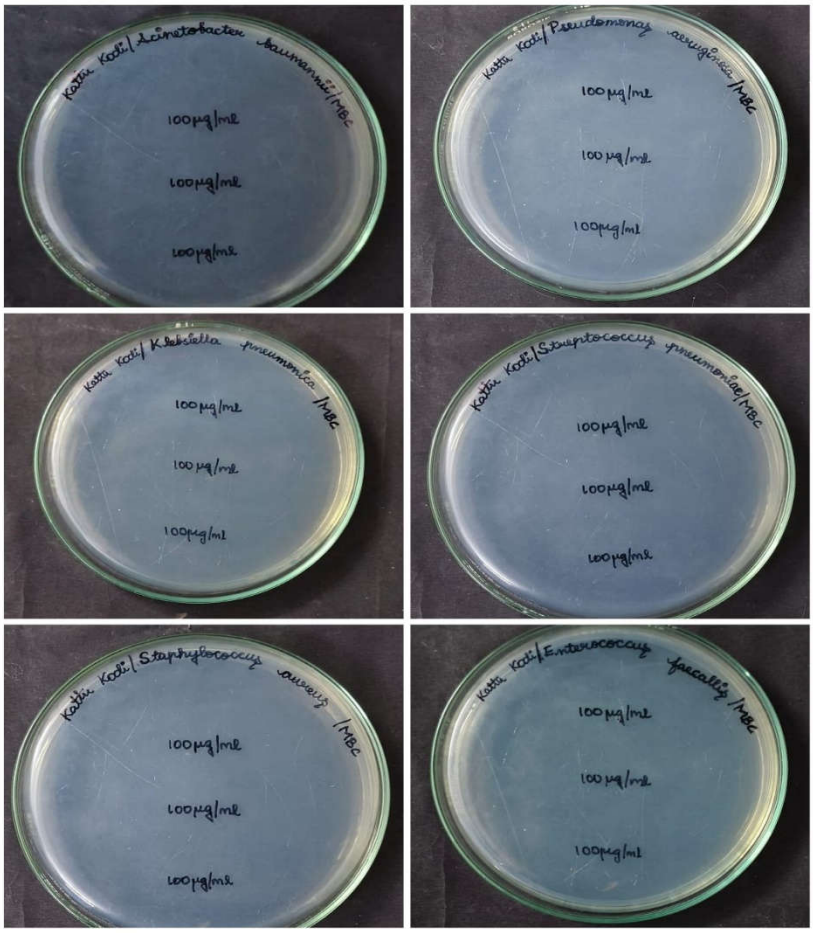

Figure 6: Determination of minimum bactericidal concentration (MBC) of *Cocculus hirsutus* extract against selected bacterial strains, showing no visible zones of inhibition at 100 µg/ml.

3.5 Biofilm analysis

The biofilm inhibition activity of *Cocculus hirsutus* extract was tested on six pathogenic organisms as shown in Table 4 and Figure 7. The extract showed some degree of inhibition activity on all six organisms. The extract inhibited mainly *Staphylococcus aureus* 61.80 % followed by *Streptococcus pneumoniae* 48.87% and *Acinetobacter baumannii* 38. 00%. *Enterococcus faecalis* was found moderate inhibitor 33.03 % while the lowest activity was on *Pseudomonas aeruginosa* 26.85% and 24.84% to *Klebsiella pneumoniae.*

Table 4: Biofilm inhibition activity of *Cocculus hirsutus* extract

S. no.	Microorganisms	Inhibition (%) (Mean ± SD)
1	*Enterococcus faecalis*	33.03 ± 0.99
2	*Pseudomonas aeruginosa*	26.85 ± 0.81
3	*Staphylococcus aureus*	61.80 ± 1.85

4	*Streptococcus pneumoniae*	48.87 ± 1.47
5	*Klebsiella pneumoniae*	24.84 ± 0.75
6	*Acinetobacter baumannii*	38.003 ± 1.14

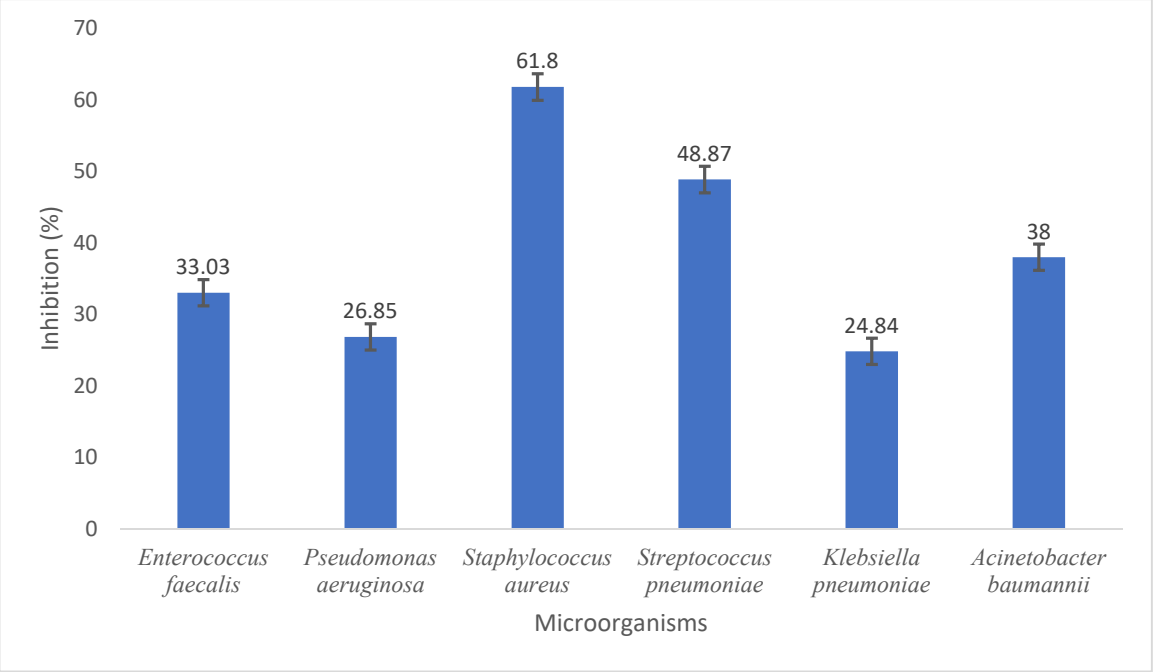

Figure 7: Biofilm inhibition by *Cocculus hirsutus* extract against selected microorganisms. Highest activity was observed at the values are expressed as mean ± SD

3.6 Surface hydrophobicity assay

The surface hydrophobicity assay shown in Table 5 and Figure 8 evaluated the reduction of surface hydrophobicity in all bacteria. Untreated bacteria, including, *Enterococcus faecalis*, *Streptococcus pneumoniae*, *Staphylococcus aureus*, *Klebsiella pneumoniae*, *Pseudomonas aeruginosa* and *Acinetobacter baumannii* showed high surface hydrophobicity which ranged from 20 to 60. The bacterial strains showed significantly reduced hydrophobicity 12 hours after treatment with *Pseudomonas aeruginosa*, the only bacteria that showed 0 hydrophobicity. *Streptococcus pneumoniae* and Enterococcus faecalis showed 6.6 and 20 hydrophobicity, respectively.

Table 5: Surface hydrophobicity (%) of bacterial strains under untreated and treated conditions.

S. no.	Microorganisms	Untreated (%) (Mean ± SD (5))	Treated (%) (Mean ± SD (5))
1	*Enterococcus faecalis*	60	20
2	*Pseudomonas aeruginosa*	20	0
3	*Staphylococcus aureus*	60	26.3
4	*Streptococcus pneumoniae*	40	6.6

5	*Klebsiella pneumoniae*	56.6	13.3
6	*Acinetobacter baumannii*	30	13.3

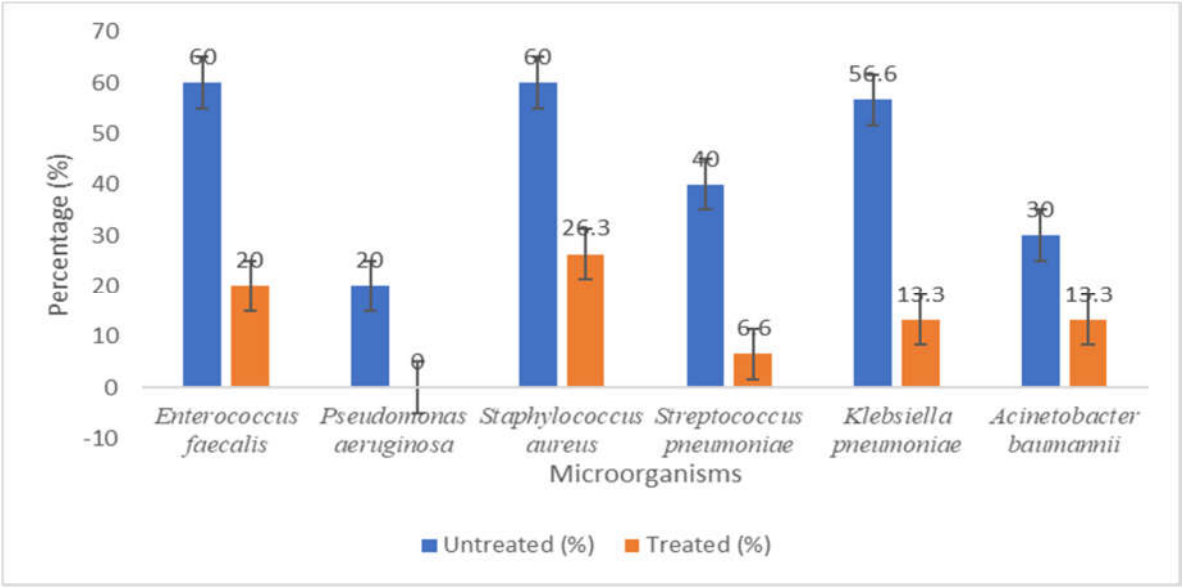

Figure 8: Surface hydrophobicity (%) of bacterial strains before and after treatment.

3.7 Membrane stability assay

The changes in optical density (OD) over time, summarized in Table 6 and displayed in Figure 9, demonstrates the effective *Acinetobacter baumannii* of the formulation treatment against the control. During the initial reading of 0 mins the untreated sample recorded an increase in OD (2.078) compared to that of the treated sample (1.178). The untreated was progressively increasing while the treated was decreasing however it is clear the treated sample was decreasing at a higher rate. During the next reading at 2 mins the untreated sample still had a high OD (1.99), while the sample treated with the formulation showed a much lower OD (0.926). This trend increased with each reading, with the untreated sample having an OD of 0.3 after 10 mins, and the treated having an OD of 0.094. This accumulated data proves the anti-bacterial activity of the formulation to be rapid and efficient.

Table 6: Effect of treatment on membrane stability at different time intervals for *Acinetobacter baumannii*

S. no.	Time interval (Minutes)	Untreated (Mean ± SD (0.05))	Treated (Mean ± SD (0.05))
1	0	2.078	1.178
2	2	1.99	0.926
3	4	0.927	0.849
4	6	0.702	0.472

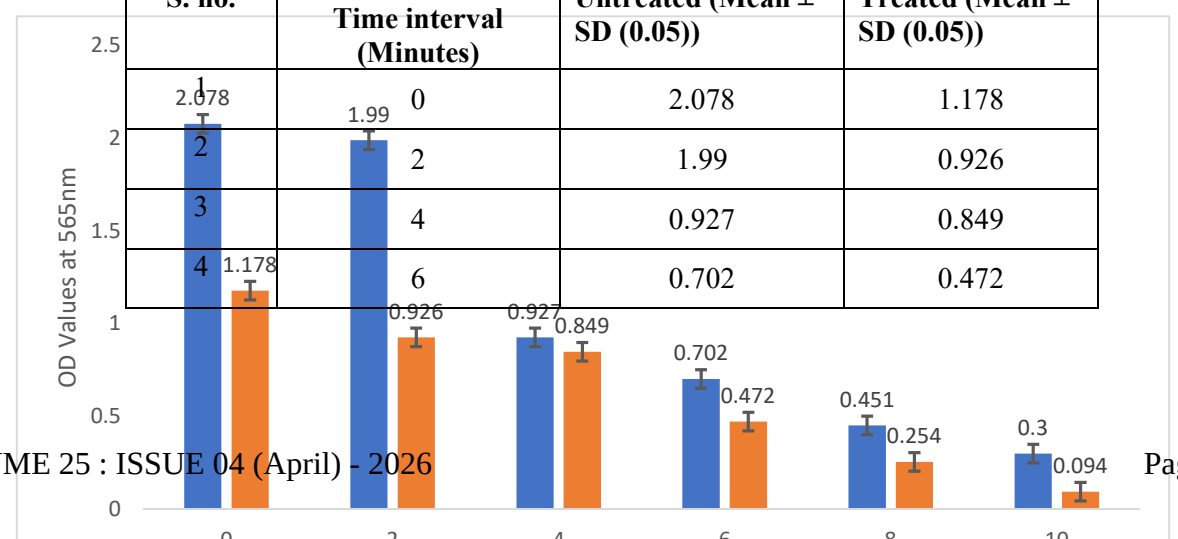

5	8	0.451	0.254
6	10	0.3	0.094

Figure 9: Membrane stability assay showing the effect of treatment over time for *Acinetobacter baumannii*

The absorbance values indicated in Table 7 and Figure 10 for membrane stability analysis shows the gradual, unexplained decrease in both untreated and treated group for *Enterococcus faecalis*, but these concentrations show far high reduction upon treatment. For 0 min initial data of 2.172 and 1.063 of untreated and treat group respectively indicate higher dependent concentration. As the time goes, the received values of both the groups show exponential decreases, but the treated groups value increases slowly. The higher reduction rate of treated group can be explained by its higher rate of killing or inactivation over the time. For 4 min, the inactivation rate of treated group (0.459) is nearly thrice of its untreated counterpart (0.75). This process of superior inactivation of treated group continued by the later time interval, where treated value reaches 0.131 and its untreated value reaches 0.217 at 10 min. The significant stable decrease of average absorbance of treated group indicates the faster efficiency of treatment for the parameter under investigation compared to untreated one. The standard deviation (+/se SD at 0.05) indicated the reliability of the measurable data obtained.

Table 7: Effect of treatment on membrane stability at different time intervals for *Enterococcus faecalis*

S. no.	Time interval (Minutes)	Untreated (Mean ± SD (0.05))	Treated (Mean ± SD (0.05))
1	0	2.172	1.063
2	2	1.984	0.898
3	4	0.75	0.459
4	6	0.414	0.317
5	8	0.302	0.282
6	10	0.217	0.131

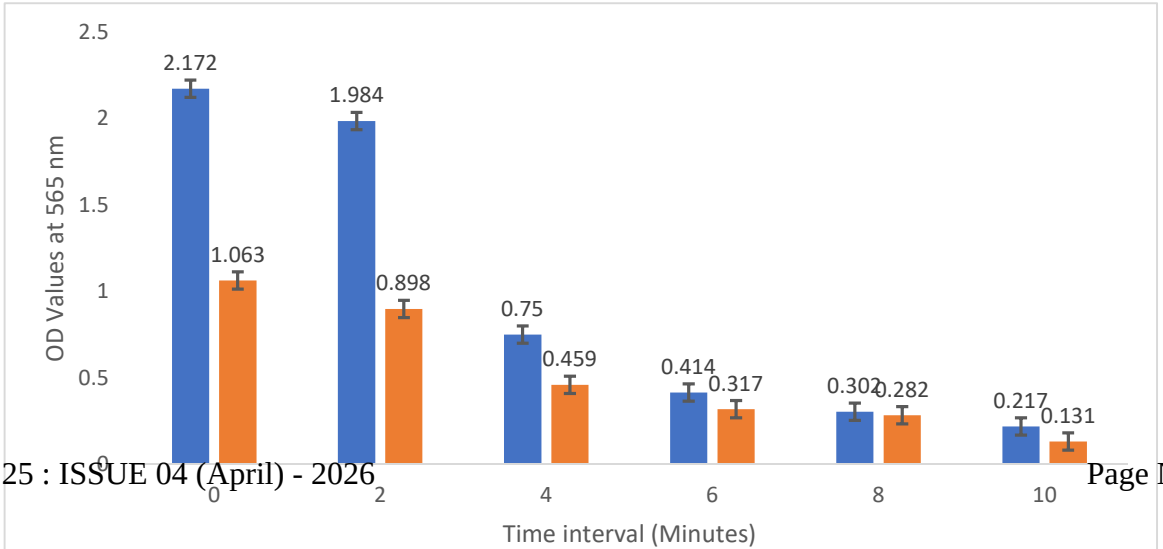

Figure 10: Membrane stability assay showing the effect of treatment over time for *Enterococcus faecalis*

The membrane stability values comparisons as showed in Table 8 and Figure 11 a gradual decrease in values were observed both in treated and untreated samples for *Klebsiella pneumoniae* but more in the treated. The values were 2.172 and 1.092 at 0 min respectively. These values fell steadily for both samples with the figures 0.836 and 0.459 at 4 min respectively. However, the results showed that the reduction of untreated sample was statistically much the same as to the treatment at later time points, a typical result show as 0.373 for the untreated and 0.217 for the treated at 10 min. Worth noting, a steady reduction was also achieved in the measured values for the treated. Moreover, the standard deviation of was within an acceptable range which confirms the reliability of the experimental results. Hence, the overall research based on the treated sample shows better performance in comparison with the untreated sample for *Klebsiella pneumoniae*.

Table 8: Effect of treatment on membrane stability at different time intervals for *Klebsiella pneumoniae*

S. no.	Time interval (Minutes)	Untreated (Mean ± SD (0.05))	Treated (Mean ± SD (0.05))
1	0	2.172	1.092
2	2	1.984	0.919
3	4	0.836	0.459
4	6	0.54	0.317
5	8	0.466	0.282
6	10	0.373	0.217

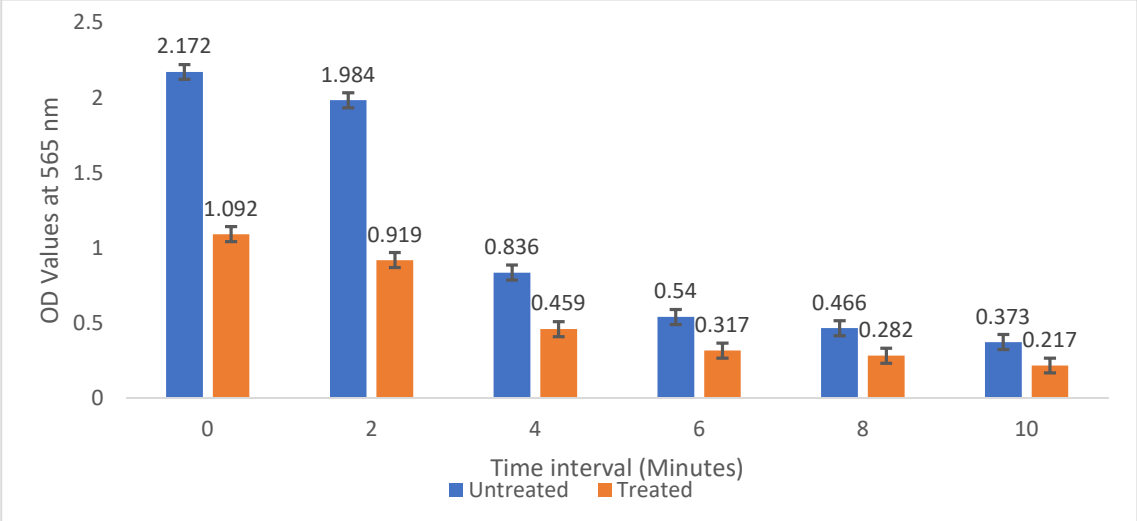

Figure 11: Membrane stability assay showing the effect of treatment over time for *Klebsiella pneumoniae*

From the membrane stability analysis for absorbance values Table 9 and Figure 12 shows when the absorbance values for both the untreated and treated samples of *Staphylococcus aureus* indicated in that both samples indicated a gradual reduction with a greater reduction in the treated sample. The untreated sample indicated a higher absorbance value than that for the treated sample (2.313 and 1.006 respectively) at 0 minutes indicating a higher value for absorbance in the untreated sample. As the sample incubation time progressed the absorbance values for the untreated sample indicated a gradual reduction but with a greater reduction in absorbance value in the treated sample, as the value at 4 minutes indicates a reduction to 0.555 in absorbance value for the treated sample compared to 0.686 in both absorbance values for the untreated sample which is a gradual transition value indicating that eventually the treated sample would have a greater reduction than the untreated sample. From 6 minutes onwards the treated samples indicated a greater reduction in absorbance value reaching 0.072 after 10 minutes. However, the untreated sample still maintained a greater value with a reduction in absorbance value after 10 minutes of 0.323. The significant reduction observed in the treated sample from 6 minutes to 10 minutes indicated that the treatment was more efficient at reducing the absorbance value.

Table 9: Effect of treatment on membrane stability at different time intervals for *Staphylococcus aureus*

S. no	**Time interval (Minutes)**	**Untreated (Mean ± SD (0.05))**	**Treated (Mean ± SD (0.05))**
1	0	2.313	1.006
2	2	1.98	0.886
3	4	0.686	0.555
4	6	0.682	0.435
5	8	0.468	0.2
6	10	0.323	0.072

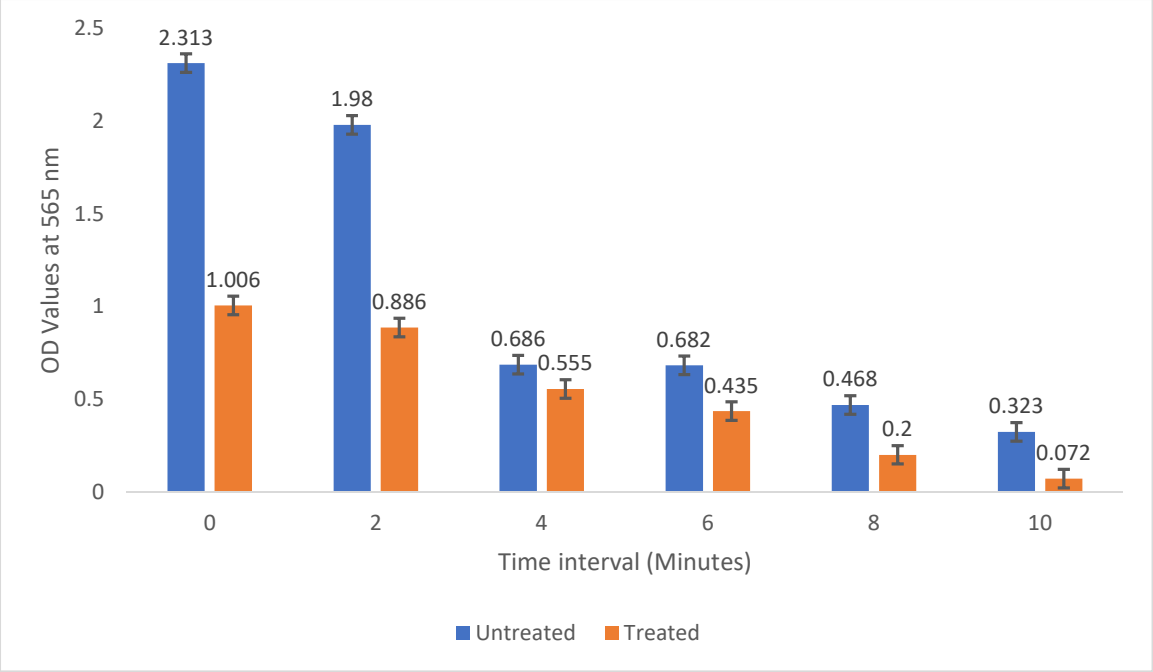

Figure 12: Membrane stability assay showing the effect of treatment over time for *Staphylococcus aureus*

Analysis of absorbance value of membrane stability analysis over time, as shown in the Table 10 and Figure 13 showed that both the untreated and treated *Streptococcus pneumoniae* samples have gradually decreased over time. The initial reading (0min) of the treated sample (1.316) has a slight variance to the untreated sample (1.98, higher overall), and then the rate of decrease over the incubations (0.643 after 4 min for the treated, compared to 0.904 for the untreated) is more rapid for the former. The trend found over time is also observed in the later time measures, with the strongest reduction after 10min being in the treated sample (0.069) as opposed to the untreated (0.388). This large difference at the later time point, further reinforces the enhanced efficiency of the treatment at a sustained time point. This drop is further facilitated by the experimental values have the table (± SD at 0.05), further illustrating the accuracy and reproducibility of this experiment.

Table 10: Effect of treatment on membrane stability at different time intervals for *Streptococcus pneumoniae*

S. no	**Time interval (Minutes)**	**Untreated (Mean ± SD (0.05))**	**Treated (Mean ± SD (0.05))**
1	0	1.98	1.316
2	2	1.298	1.071
3	4	0.904	0.643
4	6	0.769	0.378
5	8	0.664	0.198
6	10	0.388	0.069

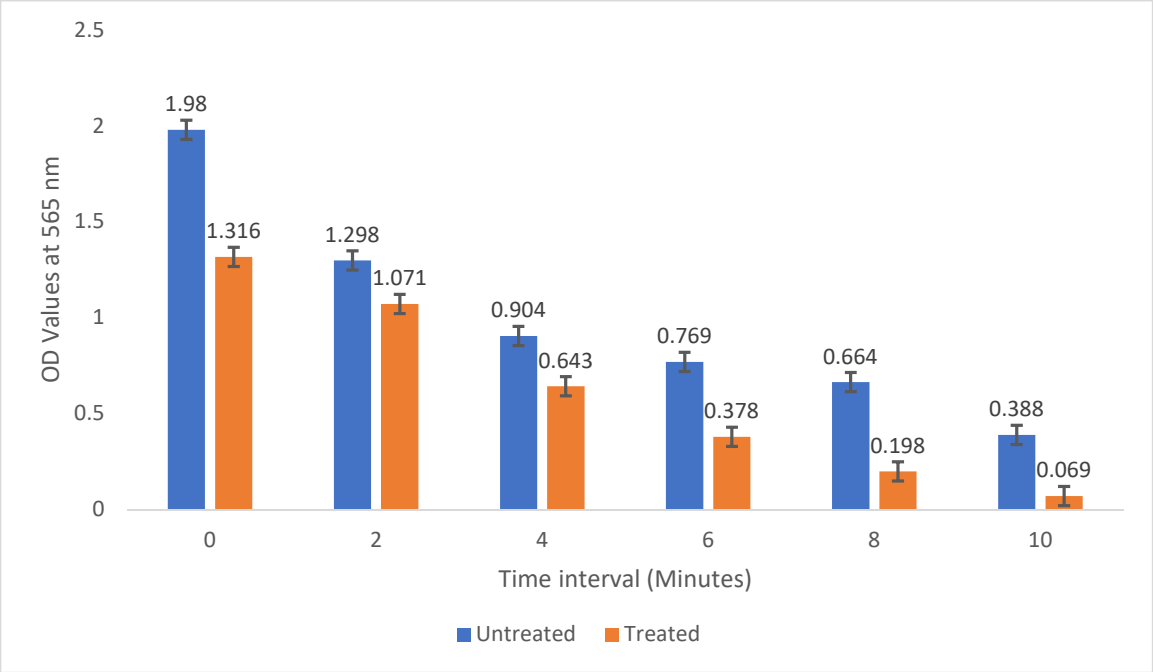

Figure 13: Membrane stability assay showing the effect of treatment over time for *Streptococcus pneumoniae*

In the Membrane stability assay evaluation of the absorbance values as shown in table 11. and figure 14. The untreated and treated samples of *Pseudomonas aeruginosa* shows a steady decrease throughout, the treated shows a much more easily attainable reduction over time in comparison to the untreated. The values at 0 min are 1.977 for the untreated and 0.96 for the treated, compared to show the difference in the two. And as the time goes on the values decrease as expected, but the reduction in the treated sample easier to produce with the values of 0.662, 0.24, 0.132 and 0.557, 0.212, 0.143 for 2, 6 and 10 min respectively. The values do not differ dramatically, but there is a notable difference in the effectiveness of the treatment in the 2 to 10 min sections and that is obvious. Standard deviation (± SD at 0.05) is included to verify the experimental data.

Table 11: Effect of treatment on membrane stability at different time intervals for *Pseudomonas aeruginosa*

S. no	**Time interval (Minutes)**	**Untreated (Mean ± SD (0.05))**	**Treated (Mean ± SD (0.05))**
1	0	1.977	0.96
2	2	1.613	0.88
3	4	0.662	0.662
4	6	0.557	0.24
5	8	0.286	0.142
6	10	0.212	0.132

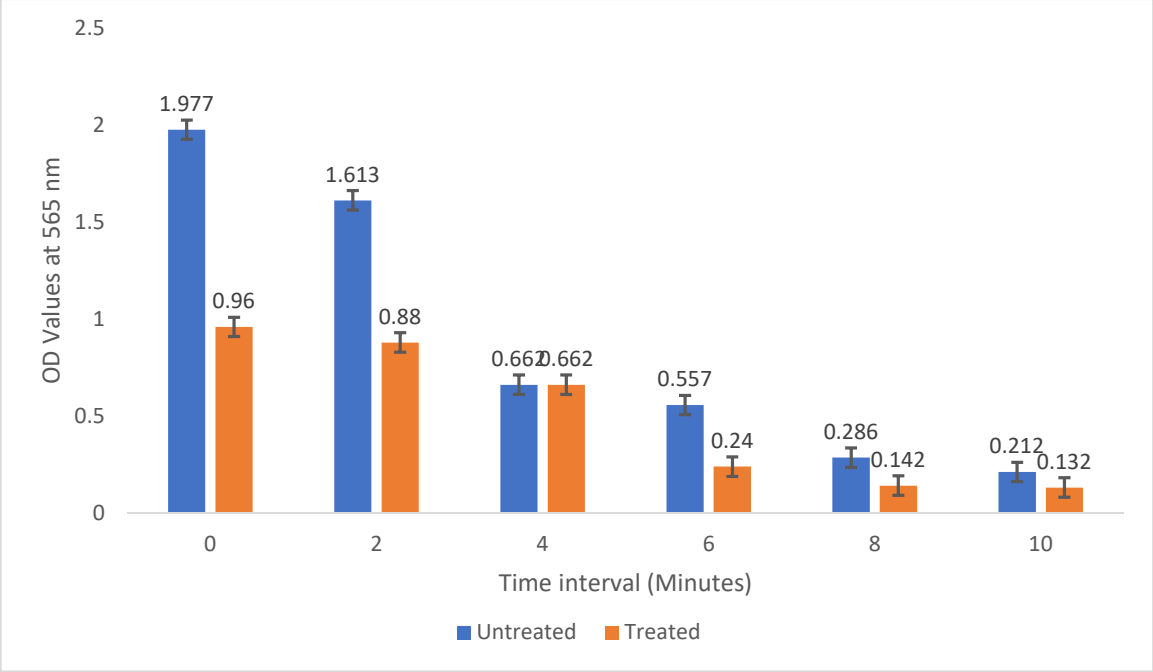

Figure 14: Membrane stability assay showing the effect of treatment over time for *Pseudomonas aeruginosa*

3.8 Docking

In this study, a molecular docking approach was employed to investigate how the compounds identified in *Cocculus hirsutus* contribute to antibacterial activity. The receptors 4RL9, 4FU0, 3RXX, 4BL2, 1QME and 3IX3 receptors have been selected for the organisms *Acinetobacter baumanii, Enterococcus faecalis, Klebsiella pneumoniae, Staphylococcus aureus, Streptococcus pneumoniae* and *Pseudomonas aeruginosa* respectively. The molecular docking analysis identified the top 10 ligands based on their lowest binding affinity values, indicating stronger interaction with the target protein. For the receptor 4RL9, Lupeol (Compound CID: 259846) showed the highest binding affinity of -8.6 kcal/mol, indicating stronger interaction with the target protein. This was followed by Butorphanol (Compound CID: 5361092) and Vitamin E (Compound CID: 14985) with binding affinity of -7.8 kcal/mol and -7.7 kcal/mol. Among all the screened receptor 4FU0, Phenytoin (Compound CID: 1775) exhibited the highest binding affinity of -9.4 kcal/mol suggesting a stable interaction. This was followed by Butorphanol (Compound CID: 5361092) and Ethyl iso-allocholate (Compound CID: 6452096) indicating excellent binding potential with -8.8 kcal/mol and -8.3 kcal/mol. The docking results with 3RXX identified top ligand Lupeol (Compound CID: 259846) with highest binding affinity of -8.5 kcal/mol. Further investigated compounds such as Ethyl iso-allocholate (Compound CID: 6452096) and Butorphanol (Compound CID: 5361092) with binding affinities -7.5 kcal/mol and -7.3 kcal/mol respectively. Among all ligands for 4BL2 receptor, Phenytoin (Compound CID: 1775) showed the highest binding affinity of -7.5 kcal/mol. Other ligands demonstrated following binding affinities are Diphenyl sulfone (Compound CID: 31386) and 1,2,3-Propanetriol, 1-acetate 2-benzoate, (2R)-) (Compound CID: 10955594) with -7.3 kcal/mol and -7.1 kcal/mol. The molecular docking analysis identified top ligand for the receptor 1QME is Phenytoin (Compound CID: 1775) with binding affinity of -7.5 kcal/mol with the active site of protein. The following ligands are Diphenyl sulfone (Compound CID: 31386) and 1,2,3-Propanetriol, 1-acetate 2-benzoate, (2R)-) (Compound CID: 10955594) with -7.3 kcal/mol and -7.1 kcal/mol which demonstrated significant binding potential. The top-performing ligands based on their binding affinities for 3IX3 was selected, Phenytoin (Compound CID: 1775) exhibited the highest binding affinity of -6.7 kcal/mol. Followed by Butorphanol (Compound CID: 5361092) and 1,2,3-Propanetriol, 1-acetate 2-benzoate, (2R)-) (Compound CID: 10955594) showed

relatively lower binding affinities with -6.2 kcal/mol and -5.9 kcal/mol. The target 4FU0 receptor showed the highest binding interaction. By the docking results of all the six receptors indicated that ligands 1775, 259846, and 5361092 consistently exhibited strong binding affinities.

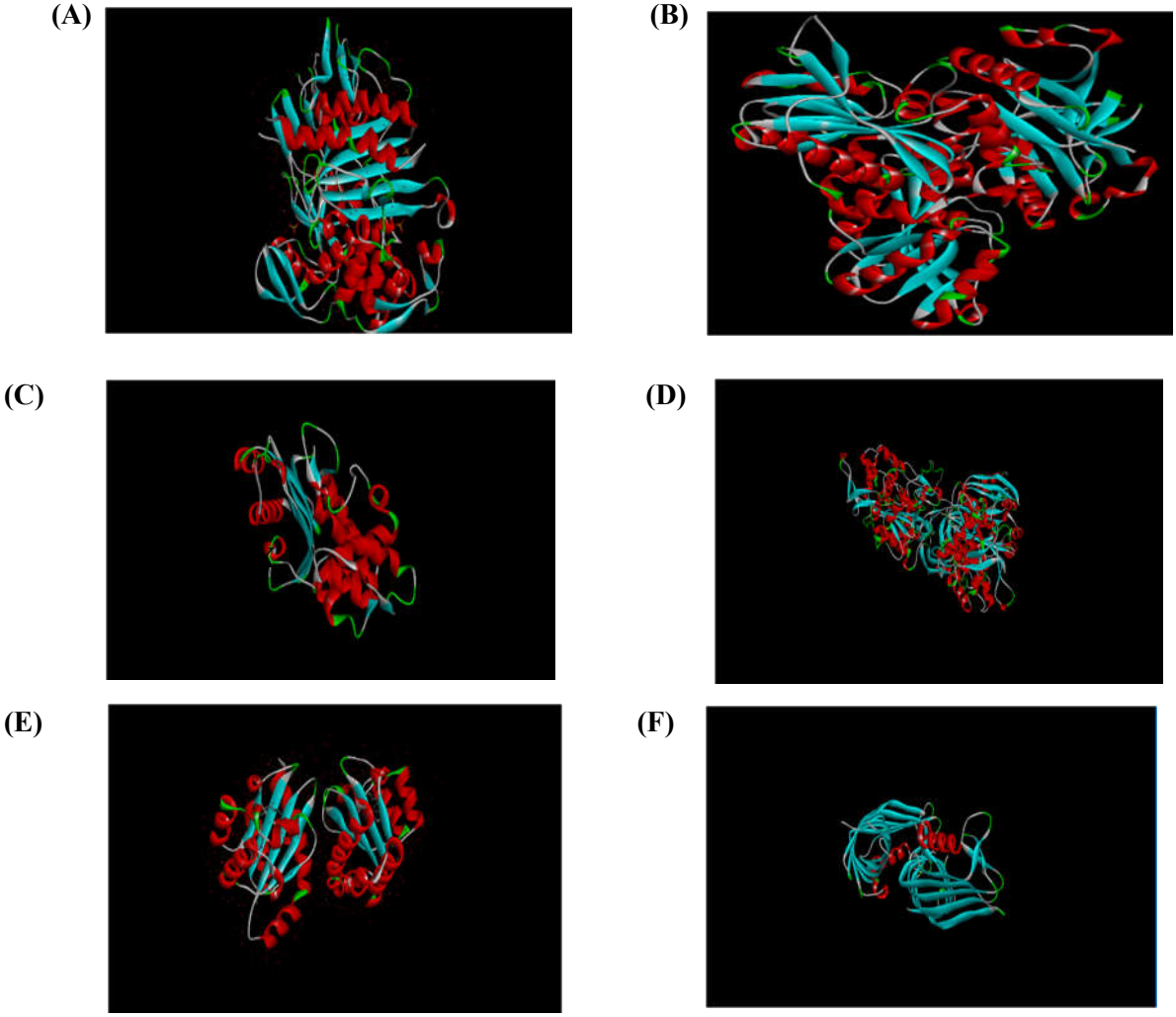

Figure 15: Microbial receptors (A) 1QME, (B) 4FUO, (C) 3RXX, (D) 4BL2, (E) 3IX3 and (F) 4RL9

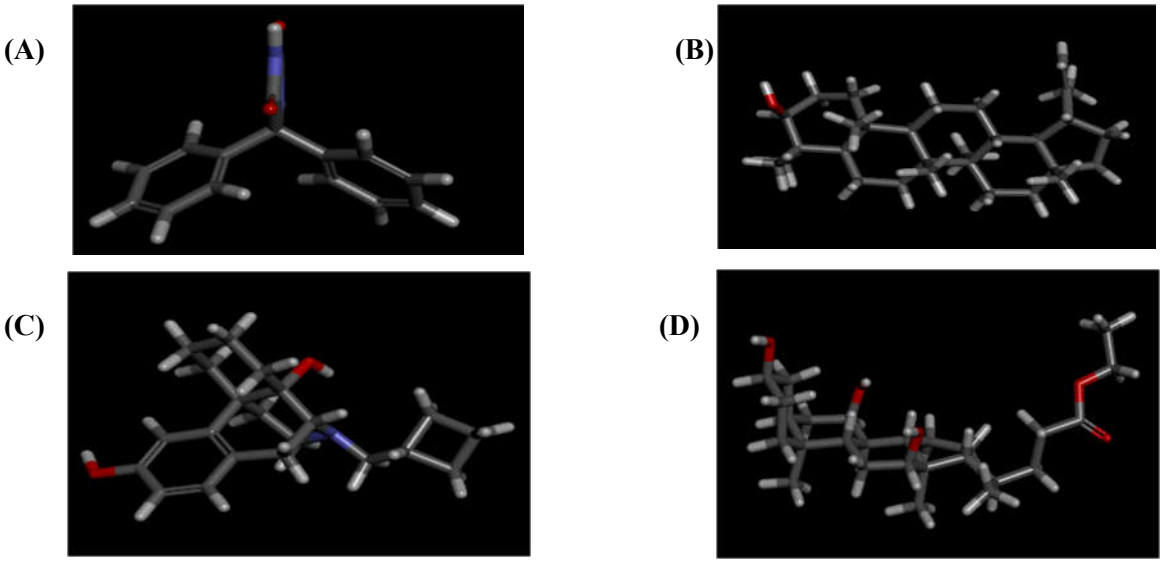

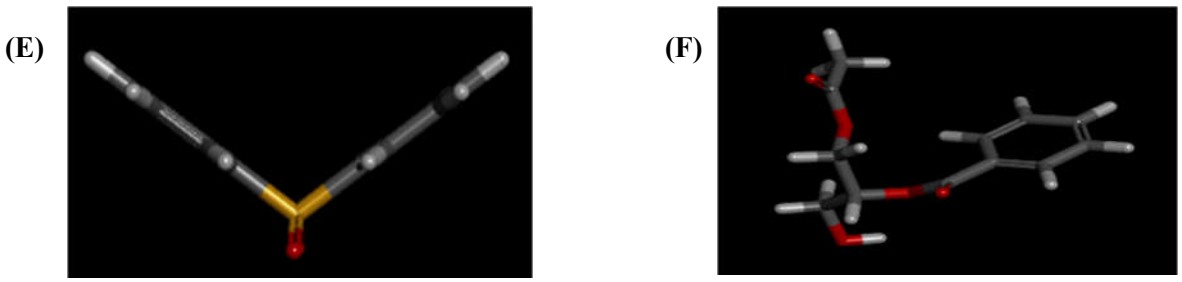

Figure 16: Ligands (A) Phenytoin – 1775, (B) Lupeol - 259846, (C) Butorphanol – 5361092, (D) Ethyliso-allocholate - 6452096, (E) Diphenyl sulfone – 31386 and (F) 1,2,3-Propanetriol, 1-acetate 2-benzoate, (2R)- - 10955594

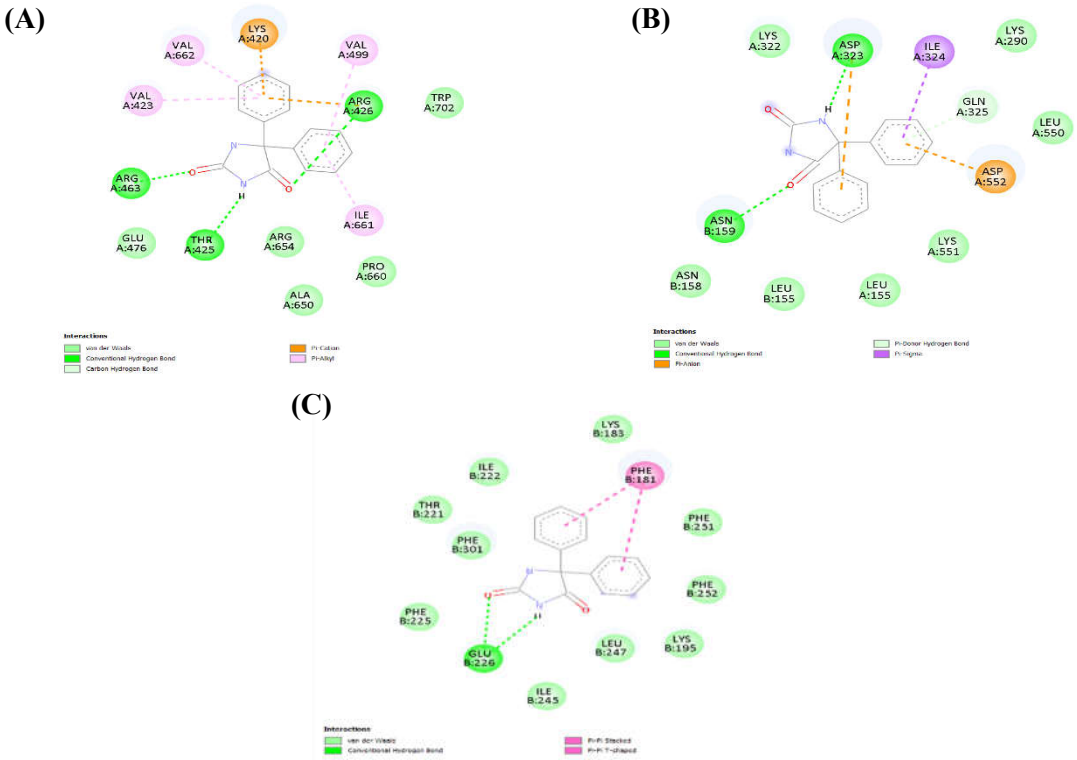

Figure 17: A 2D representation of a ligand (1775 – Phenytoin) binding to a receptors active site, showing intermolecular interactions like hydrogen bonds (A) Receptor - 1QME, (B) Receptor – 4BL2, and (C) Receptor – 4FU0

3.9 ProTox II

The toxicity test was evaluated through computational analysis and is proved that the phenytoin compound is used as the primary bioactive compound or reference compound to determine the potential for the medicinal use of this plant. The toxicological profiling of the bioactive compounds found within *Cocculus hirsutus*, specifically with respect to the anticonvulsant compound Phenytoin, demonstrates a highly positive and favorable toxicology and pharmacokinetic profile. The compound, based on this analysis, demonstrates a molecular weight of 252.27 Da and a partition coefficient (logP) of 2.43, indicating a highly positive lipophilicity that is required to traverse the blood-brain barrier, a requisite for neurological applications for *Cocculus hirsutus*. The acute toxicity analysis of this compound shows that, with an LD50 value of 150 mg/kg, this compound would be classified in Toxicity Class 3. However, from the "Inactive Cluster" analysis, we find that this compound has a remarkably low chance of causing systemic side effects, with a high probability that this compound will be inactive for a variety of different types of toxicity, such as Immunotoxicity (0.99), Cardiotoxicity (0.88), and Mutagenicity (0.86). The compound has a high probability of being orally bioavailable, and a high level of structural

stability, as evidenced by a Topological Polar Surface Area (TPSA) of 58.2 and a relatively low number of rotatable bonds (2). The compound found in Cocculus hirsutus has a high probability of being therapeutically active, while at the same time having a high probability of being inactive regarding several different stress response mechanisms, including p53 and MMP.

(A)

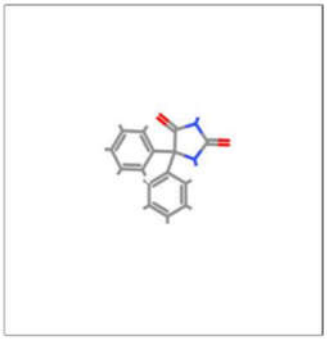

Predicted LD50: 150mg/kg

Predicted Toxicity Class: 3

1 2 3 4 5 6

Average similarity: 100%

Prediction accuracy: 100%

Name	Phenytoin
Molweight	252.27
Number of hydrogen bond acceptors	4
Number of hydrogen bond donors	2
Number of atoms	19
Number of bonds	21
Number of rotable bonds	2
Molecular refractivity	77.5
Topological Polar Surface Area	58.2
octanol/water partition coefficient(logP)	2.43

(B)

Classification	Target	Shorthand	Prediction	Probability
Organ toxicity	Nephrotoxicity	nephro	Inactive	0.70
Organ toxicity	Cardiotoxicity	cardio	Inactive	0.88
Toxicity end points	Immunotoxicity	immuno	Inactive	0.99
Toxicity end points	Mutagenicity	mutagen	Inactive	0.86
Toxicity end points	Cytotoxicity	cyto	Inactive	0.73
Tox21-Nuclear receptor signalling pathways	Aryl hydrocarbon Receptor (AhR)	nr_ahr	Inactive	0.95
Tox21-Nuclear receptor signalling pathways	Estrogen Receptor Alpha (ER)	nr_er	Inactive	0.97
Tox21-Nuclear receptor signalling pathways	Peroxisome Proliferator Activated Receptor Gamma (PPAR-Gamma)	nr_ppar_gamma	Inactive	0.98
Tox21-Stress response pathways	Nuclear factor (erythroid-derived 2)-like 2/antioxidant responsive element (nrf2/ARE)	sr_are	Inactive	0.98
Tox21-Stress response pathways	Mitochondrial Membrane Potential (MMP)	sr_mmp	Inactive	0.90
Tox21-Stress response pathways	Phosphoprotein (Tumor Supressor) p53	sr_p53	Inactive	0.96
Molecular Initiating Events	GABA receptor (GABAR)	mie_gabar	Inactive	0.96
Molecular Initiating Events	Glutamate N-methyl-D-aspartate receptor (NMDAR)	mie_nmdar	Inactive	0.92
Metabolism	Cytochrome CYP2C19	CYP2C19	Inactive	0.85
Metabolism	Cytochrome CYP2C9	CYP2C9	Inactive	0.61
Metabolism	Cytochrome CYP2D6	CYP2D6	Inactive	0.76
Metabolism	Cytochrome CYP3A4	CYP3A4	Inactive	0.97

(C)

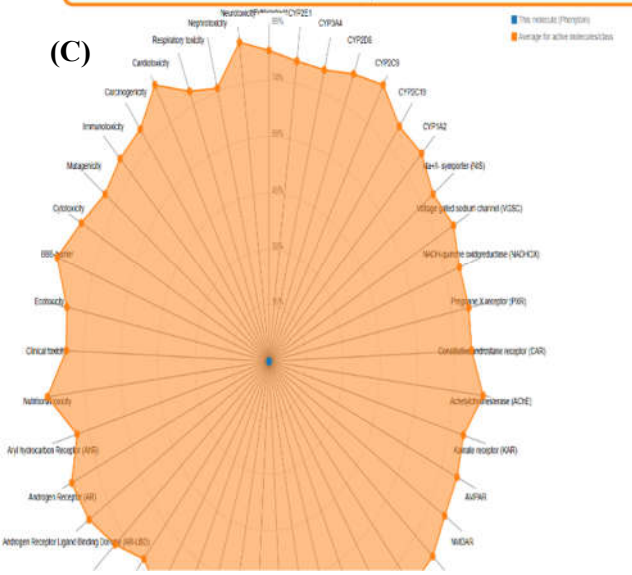

(D)

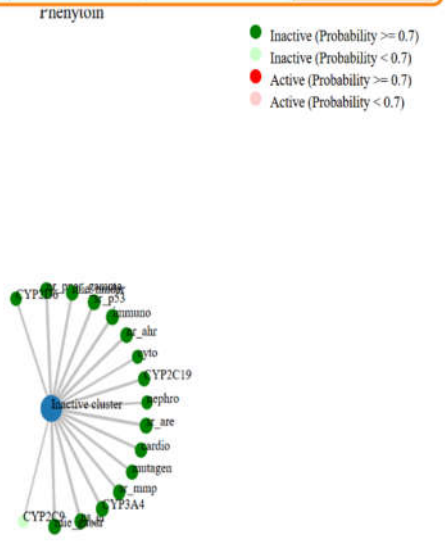

Figure 18: ProTox II *In-silico* analysis (A) Phenytoin compound, (B) Toxicity prediction, (C) Radar chart, and (D) Network chart

3.10 pkCSM

The output of a computational toxicity prediction analysis was evaluated using RADAR for a chemical compound. On the left side, the molecular structure is illustrated, showing a complex multi-ring framework with several attached functional groups, suggesting a steroid-like configuration. Below the structure, key molecular properties are provided, including a molecular weight of 426.729, a high logP value of 8.0248 indicating strong lipophilicity, one rotatable bond, and minimal hydrogen bond acceptors and donors, along with a surface area of 192.398. On the right side, a detailed toxicity profile is displayed, highlighting that the compound is non-mutagenic as it shows no AMES toxicity and is also non-hepatotoxic and non-sensitizing to skin. However, it is predicted to act as an hERG II inhibitor, which may indicate potential cardiotoxic effects. The compound demonstrates moderate oral toxicity based on rat acute (LD50 = 2.563 log mol/kg) and chronic (LOAEL = 0.89 log mg/kg, bw/day) values. Additionally, ecological toxicity parameters such as *Tetrahymena pyriformis* toxicity (0.316 log µg/L) and minnow toxicity (-1.696 log mM) suggest some level of environmental impact. Overall, the compound appears relatively safe in terms of mutagenicity and liver toxicity.

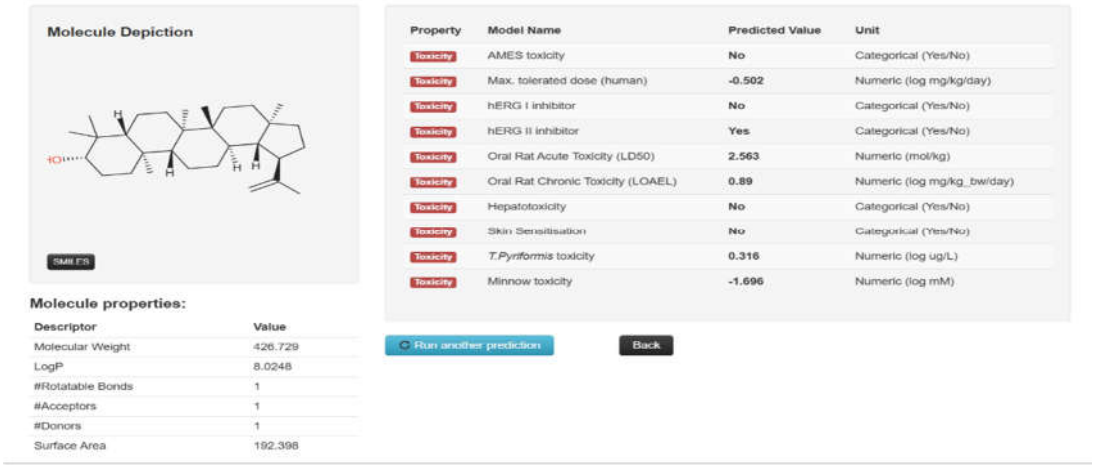

Figure 19: *In-silico* analysis of toxicity in pkCSM

4. Conclusion

The current study provides the evaluation of the *Cocculus hirsutus* with phytochemicals, moderate anti-diabetic activity, and notable anti-microbial and biofilm inhibition against diabetic wound healing. These findings validate its traditional use for diabetic wound management highlighting its potential by plant-based therapeutic.

Acknowledgement

This research is a part of B. Tech Biotechnology, the Project work of the first and second authors.

Disclosure statement

The authors have declared no conflict of interest.

Reference:

1. Mohamed Elshikh, Syed Ahmed, Scott Funston, Paul Dunlop, Mark McGaw, Roger Marchant, Ibrahim M Banat. Resazurin-based 96-well plate microdilution method for the determination of minimum inhibitory concentration of biosurfactants. 2016. doi: 10.1007/s10529-016-2079-
2. Ramya, P., Vasanth, P. M., Prasad, P. V., & Babu, S. V. (2019). Qualitative phytochemical screening tests of Alpinia galanga L. *World Journal of Pharmaceutical Research*, *8*(5), 1064-1077.

3. Lourenço, B. J., Massina, C. F. O., João, A. A., Cuinica, L. G., & Vintuar, P. A. (2024). Identification Data of secondary metabolites and Antibacterial Action of leaf extract of Lantana camara L. on multidrug-resistant microorganisms. *Data in Brief*, *54*, 110338.
4. Yunitasari, N., Swasono, R. T., Pranowo, H. D., & Raharjo, T. J. (2022). Phytochemical screening and metabolomic approach based on Fourier transform infrared (FTIR): Identification of α-amylase inhibitor metabolites in Vernonia amygdalina leaves. *Journal of Saudi Chemical Society*, *26*(6), 101540.
5. Wiraswati, H. L., Pradini, G. W., Fauziah, N., Laelalugina, A., Arimdayu, A. R., Supandi, S., ... & Ma'ruf, I. F. (2024). Biological potential of eight medicinal plants collected in the restored landscape after mining in South Kalimantan. *Discover Applied Sciences*, *6*(6), 308.
6. Godlewska, K., Pacyga, P., Najda, A., & Michalak, I. (2023). Investigation of chemical constituents and antioxidant activity of biologically active plant-derived natural products. *Molecules*, *28*(14), 5572.
7. S. Sazada, A. Verma, A. A. Rather, F. Jabeen, andM. K. Meghvansi, "Preliminary phytochemicals analysis ofsome important medicinal and aromatic plants," Advances in Biological Research, vol. 3, pp. 188–195, 2009.
8. Samar, J., Butt, G. Y., Shah, A. A., Shah, A. N., Ali, S., Jan, B. L., ... & Hussaan, M. (2022). Phycochemical and biological activities from different extracts of Padina antillarum (Kützing) Piccone. *Frontiers in Plant Science*, *13*, 929368.
9. Rahmi, N. S., Maharani, M. P., Irianto, K., Rizky, I. A., Fadillah, A. P., & Firdaus, M. (2025). Green Extraction of Peppermint as an Antibacterial Agent in Thermo Suganya sensitive Hydrogel for Diabetic Wound Healing. ChemistrySelect,
10. Rachel C. Selvaraj, Gino Cioffi, Kristin A. Waite, Sarah S. Jackson and Jill S. Barnholtz-Sloa. Pan-Cancer Analysis of Age and Sex Differences in Cancer Incidence and Survival in the United States, 2001–2020. doi.org/10.3390/cancers17030378.
11. Mel Rosenberg. Microbial adhesion to hydrocarbons: twenty-five years of doing MATH. 2006. doi: 10.1111/j.1574-6968.2006.0029.x.. Microbiology and Molecular Biology Reviews, 74, 417-433 (doi.org/10.1128/MMBR.00016-10).
12. N. Jayachandra Reddy, D. Nagoor Vali, M. Rani, S. Sudha Rani. Evaluation of antioxidant, antibacterial and cytotoxic effects of green synthesized silver nanoparticles by Piper longum fruit. 2014. doi.org/10.1016/j.msec.2013.08.039.
13. Fatemeh Esnaashari,Dorna Rostamnejad, Hossein Zahmatkesh, Hojjat Zamani. In vitro and in silico assessment of anti-quorum sensing activity of Naproxen against Pseudomonas aeruginosa. 2023. doi:10.1007/s11274-023-03690-5
14. Mellini, M., Di Muzio, E., D'Angelo, F., Baldelli, V., Ferrillo, S., Visca, P., ... & Rampioni, G. (2019). In silico selection and experimental validation of FDA-approved drugs as anti-quorum sensing agents. *Frontiers in Microbiology*, *10*, 2355.
15. Pouget, C., Dunyach-Remy, C., Pantel, A., Schuldiner, S., Sotto, A., & Lavigne, J. P. (2020). Biofilms in diabetic foot ulcers: significance and clinical relevance. *Microorganisms*, *8*(10), 1580.
16. Darvishi, S., Tavakoli, S., Kharaziha, M., Girault, H. H., Kaminski, C. F., & Mela, I. (2022). Advances in the sensing and treatment of wound biofilms. *Angewandte Chemie International Edition*, *61*(13), e202112218.
17. Anita, H., Manoj, A., Arunagirinathan, N., Rameshkumar, M. R., Revathi, K., Selvam, R., ... & AbdelGawwad, M. R. (2023). Bacterial etiology, antibiotic resistance profile and foot ulcer associated amputations in individuals with Type II diabetes mellitus. *Journal of King Saud University-Science*, *35*(8), 102891.
18. Logesh, R., Das, N., Adhikari-Devkota, A., & Devkota, H. P. (2020). Cocculus hirsutus (L.) W. Theob.(Menispermaceae): a review on traditional uses, phytochemistry and pharmacological activities. *Medicines*, *7*(11), 69.
19. Abbagoni, S., Edupuganti, S., & Rani, G. J. (2021). Phytochemical and antioxidant screening of Cocculus hirsutus and Calycopteris floribunda. *International journal of health sciences*, 532-540.

20. Nayak, S., & Singhai, A. K. (2003). Antimicrobial activity of the roots of Cocculus hirsutus. *Ancient science of life*, *22*(3), 101-105.
21. Kalirajan, A., Michael, J. S. A., Singh, A. J. A. R., & Padmalatha, C. (2011). Antimicrobial and wound healing studies on the extracts of *Cocculus hirsutus* (Linn). *International Journal of Applied Biology and Pharmaceutical Technology*, *2*(1), 62–66.
22. Badole, S., Patel, N., Bodhankar, S., Jain, B., & Bhardwaj, S. (2006). Antihyperglycemic activity of aqueous extract of leaves of *Cocculus hirsutus* (L.) Diels in alloxan-induced diabetic mice. *Indian Journal of Pharmacology*, *38*(1), 49–53. https://doi.org/10.4103/0253-7613.19857.
23. Meng, X.-Y., Zhang, H.-X., Mezei, M., & Cui, M. (2011). Molecular docking: A powerful approach for structure-based drug discovery. *Current Computer-Aided Drug Design*, *7*(2), 146–157. https://doi.org/10.2174/157340911795677602.
24. Nasr, M. N. A., El-Sherbiny, G. M., Kamel, Z., El-Sherif, A. A., & Abdallah, M. (2022). Phytochemical screening, in silico molecular docking, ADME properties, and in vitro antioxidant, anticancer, and antidiabetic activity of the marine halophyte *Suaeda maritima* (L.) Dumort. *ACS Omega*, *8*(46), 44133–44148. https://doi.org/10.1021/acsomega.3c05591.
25. Thamaraiselvi, K., Gomathi, E., & Ravikumar, S. (2021). In silico molecular docking on bioactive compounds from Indian medicinal plants against type 2 diabetic target proteins. *International Journal of Pharmaceutical Sciences and Research*, *12*(5), 2799–2808. https://doi.org/10.13040/IJPSR.0975-8232.12(5).2799-08.